Femtosecond streaking of electron diffraction patterns to study structural dynamics in crystalline matter

Eichberger, M.; Erasmus, N.; Haupt, K.; Kassier, G.; von Flotow, A.; Demsar, J.; Schwoerer, H.

Published in:
Applied Physics Letters

DOI:
10.1063/1.4798518

Femtosecond streaking of electron diffraction patterns to study structural dynamics in crystalline matter

M. Eichberger, N. Erasmus, K. Haupt, G. Kassier, A. von Flotow, J. Demsar, and H. Schwoerer

Citation: Appl. Phys. Lett. **102**, 121106 (2013); doi: 10.1063/1.4798518
View online: https://doi.org/10.1063/1.4798518
View Table of Contents: http://aip.scitation.org/toc/apl/102/12
Published by the American Institute of Physics

Femtosecond streaking of electron diffraction patterns to study structural dynamics in crystalline matter

M. Eichberger,[1,a)] N. Erasmus,[2,a)] K. Haupt,[2] G. Kassier,[2] A. von Flotow,[2] J. Demsar,[1,3] and H. Schwoerer[2]
[1]*Department of Physics and Center of Applied Photonics and Zukunftskolleg, University of Konstanz, D-78457 Konstanz, Germany*
[2]*Laser Research Institute, Department of Physics, University of Stellenbosch, 7600 Stellenbosch, South Africa*
[3]*Ilmenau University of Technology, Institute of Physics, D-98693 Ilmenau, Germany*

(Received 19 December 2012; accepted 14 March 2013; published online 26 March 2013)

A table-top femtosecond, non-relativistic, electron diffraction setup is combined with a low-jitter, photo-triggered streak camera to follow the optically induced structural dynamics in complex solids. A temporal resolution of 550 fs is experimentally demonstrated, while the route to streaking with sub-250 fs temporal resolution is outlined. The streaking technique allows for parallel capturing of temporal information as opposed to the serial data acquisition in a conventional scanning femtosecond electron diffraction. Moreover, its temporal resolution is not corrupted by increasing the number of electrons per pulse. Thus, compared to the conventional scanning approach, a substantial increase in signal-to-noise ratio (SNR) can be achieved. These benefits are demonstrated by studying a photo-induced charge density wave phase transition in $4H_b$-$TaSe_2$ using both methods. Within the same data acquisition time a three-fold increase in SNR is achieved when compared to the scanning method, with ways for a further improvement outlined. © *2013 American Institute of Physics*. [http://dx.doi.org/10.1063/1.4798518]

Dynamics in matter on their intrinsic atomic timescale have been experimentally investigated extensively over the past two decades by femtosecond laser spectroscopy. Monitoring the evolution of optically allowed transitions, specifically electronic excitations, has revealed a wealth of coherent and incoherent photo-physics and photo-chemistry. Recently x-ray and electron diffraction techniques with sub-picosecond resolution have been developed for direct observation of sub-Ångström atomic dynamics in crystalline matter.[1–5] Both techniques, i.e., ultrafast x-ray diffraction with laser driven sources or free electron lasers and Femtosecond Electron Diffraction (FED), still hold great maturing potentials. Higher flux, increased signal-to-noise ratio (SNR), and higher temporal resolution are the main targets for improvement. While sub-picosecond x-ray and electron diffraction essentially strive for similar observations, FED has the appeal of experimental compactness and high scattering efficiency of electrons in matter.

One of the major hurdles in femtosecond electron diffraction at non-relativistic energies is achieving sub-picosecond temporal resolution: When increasing the electron number to above 10^3 electrons per pulse, space charge repulsion dramatically broadens the electron bunch laterally and longitudinally as it propagates towards the sample.[6] Thus one tries to keep the experimental setup as compact as possible and the electron number low. However, a meaningful diffraction pattern with sufficient signal-to-noise ratio requires 10^6–10^7 electrons calling for extensive averaging and long data collection times. Another challenge in the case of non-reversible, photo-triggered dynamics is the necessity of replacing the sample with a fresh one after each shot. Nevertheless, FED has been successfully applied to studies of ultrafast irreversible-reversible phase transitions in, e.g., metals or transition metal dichalcogenides.[1–3,5,7,8] Exciting approaches to counteract the problem of Coulomb repulsion while accommodating large electron numbers have also been developed recently. While re-compressing the temporally broadened electron pulse with radio-frequency (RF) cavities has been governed by substantial timing jitter between the RF-electronics and the electron pulse, recent experimental work demonstrated an overall temporal resolution of 400 fs over the course of an experiment.[9,10] Photo-triggered open cavity compressors have the intrinsic advantage of a sub 100 fs timing jitter, experimentally demonstrating a temporal resolution of less than 750 fs.[11]

In this letter we demonstrate an alternative solution to achieving sub-picosecond resolution and improved signal-to-noise ratio, which utilizes long electron pulses to its advantage. As in the conventional pump-probe setup a femtosecond laser pulse is used to excite the sample, but instead of a short electron pulse an electron pulse of several picoseconds acts as the probe. In this concept different temporal components of the electron pulse are diffracted off the sample at different times relative to the photo-excitation pulse (see Fig. 1). The different temporal components of the diffracted signal are then spatially separated on the detector screen by means of the rapidly changing electric field in a photo-triggered, electron streak camera[12] (see Figs. 1 and 2). The transient signal can then be obtained by analyzing the intensity profile of the streaked image. The technique of streaking an electron pulse to spatially separate different temporal components was already proposed in the 1980s[13] with picosecond resolution. Recently it was implemented in time resolved electron diffraction with relativistic electrons using an electronically synchronized high-Q RF-cavity based streak camera.[14] Photoinduced melting of gold on a 10 ps time scale was observed in single shot mode.[15]

[a)]M. Eichberger and N. Erasmus contributed equally to this work.

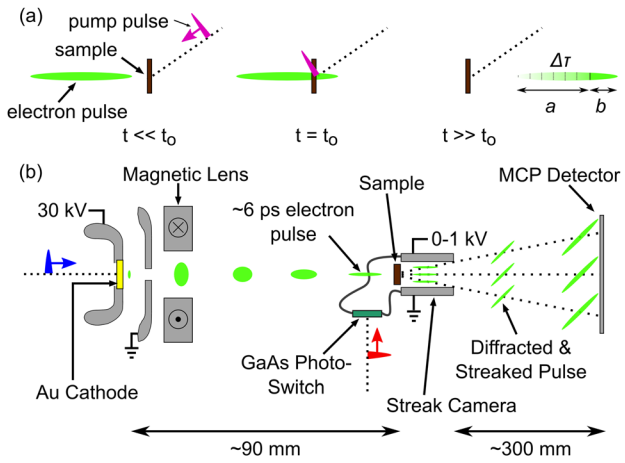

FIG. 1. (a) Principle of streaked diffraction: t_0 is chosen such that section *b* of the long electron pulse passes through unpumped sample while section *a* of the pulse records the temporal evolution of the sample's structure after it has been pumped. (b) These slices of the probe pulse are afterwards spatially separated via a photo-triggered streak camera on to the detector screen.

Our streaked electron diffraction setup combines a femtosecond non-relativistic electron gun[8] with a photo-triggered, low jitter streak camera.[12] The low jitter of the streak camera allows for maintaining sub-picosecond temporal resolution in accumulation mode, i.e., while integrating over an arbitrary number of shots. We apply the technique to track the complex dynamics in the charge density compound (CDW) $4H_b$-$TaSe_2$ excited with intense near-infrared pulses. Despite the small changes and weak satellite reflection intensities the dynamics of the photo-induced phase transition between the commensurate and incommensurate CDW phase could be mapped out within one hour data acquisition.

In this experiment 200 fs laser pulses ($\lambda = 775$ nm, repetition rate 1 kHz) are divided into three paths: one drives the electron gun and generates electron pulses, one excites the sample, and one triggers the streak camera. After exiting the electron gun, the 30 keV electrons are focused by a magnetic lens through the sample and onto a micro channel plate amplified phosphor screen; the scintillating screen is imaged onto the charge coupled device (CCD) camera by a macro lens. Sample and streak camera are placed 90 mm beyond the magnetic lens to allow the 20 000 electrons per pulse to Coulomb-expand to a pulse duration of ~6 ps (see Fig. 1(b)).

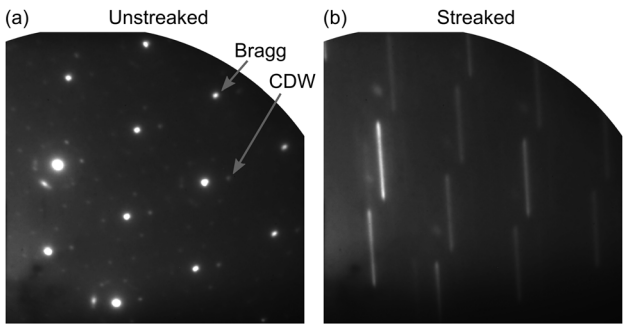

FIG. 2. Scanned and streaked diffraction patterns: (a) diffraction pattern of 4 H_b-$TaSe_2$ with the streak camera voltage switched off. The layered hexagonal crystal structure results in hexagonally arranged, bright Bragg diffraction peaks. The CDW supermodulation results in the appearance of six weak satellite reflections surrounding each Bragg reflection, referred to as CDW reflections. Panel (b) shows the streaked diffraction pattern.

The 90 nm thick 4 H_b-$TaSe_2$ sample is mounted directly on the streak camera's 100 μm entrance aperture located 2 mm in front of the streaking plates ($4 \times 4\,mm^2$, 600 μm separation). This configuration allows several diffraction orders to be streaked without being clipped by the plates. A GaAs photo-switch ($3 \times 6\,mm^2$) is mounted directly at one side of the streak plates. The plates are charged by 700 V with a 20 ns long high voltage pulse. Exciting the GaAs switch with the laser pulse triggers the discharge of the streak plates yielding a damped oscillating electric field at 6 GHz with a maximum rate of change of electric field of 30 $\frac{kV}{m\,ps}$. The trigger laser pulse is timed such that the temporal center of the electron pulse passes the streak camera at the $E = 0$ position (zero deflection) of the first oscillation. This allows streaking to occur during the linear part of the transient change in electric field. The pump pulse counter-propagates the electron pulse and travels through the streak plates before exciting the sample. The fluence on the sample was set to 3 mJ/cm^2, which is sufficient to drive the phase transition and hence leads to the complete disappearance of the CDW diffraction satellites. The pump laser pulse was delayed such that it excites the sample after roughly one fifth of the electron pulse has passed through the sample as sketched in Fig. 1(a). Once the respective timing of the three pulses has been adjusted, no physical movement of any part of the setup is required, thus eliminating a potential noise source.

Fig. 2(a) displays a diffraction pattern of $4H_b$-$TaSe_2$. Here the bright peaks are the Bragg peaks of the underlying host lattice, while the $(\sqrt{13} \times \sqrt{13})$R13.9 CDW superstructure appearing below 410 K gives rise to 6 faint peaks (referred to as CDW peaks) surrounding each of the bright lattice reflections.[16] To extract the transients from the streaked diffraction patterns as seen in Fig. 2(b), all streaks were superimposed for improved SNR (see Fig. 3(a)). In order to retrieve the transient changes in the diffraction intensity, the diffraction profile in vertical direction of the dotted rectangular boxes is analyzed for pumped (I_p) and unpumped (I_{up}) images. The transient signals plotted in Fig. 4 represent the relative changes in scattering intensity: $\Delta I/I_0 = (I_p - I_{up})/I_{up}$. The obtained data can be qualitatively explained by considering two photo triggered processes: (i) the photoinduced changes in the interatomic potential launches a coherent atomic motion towards the unmodulated phase and (ii) a rapid transfer of energy into the phonon subsystem gives rise to a conventional Debye-Waller effect. Since (i) affects the lattice and superlattice reflections in the opposite way,[5,8] the traces are fitted with the function: $\Delta I/I_0(t) = C_1(1 - \exp(-t/\tau_{coh}))$ $+C_2(1 - \exp(-t)/\tau_{icoh})$, with $C_1, C_2 < 0$ for the case of the CDW reflections and $C_1 > 0, C_2 < 0$ to fit the dynamics of Bragg reflections (see Ref. 8) for details on the model. This function has been convoluted with the measured experimental temporal resolution of the setup of 550 fs. The time constants used in the fit model are the extracted time constants from the conventional scanning experiment,[8] $\tau_{coh} = 150$ fs and $\tau_{icoh} = 500$ fs, and demonstrate the good agreement of the results from both techniques. For comparison, panels (b) and (d) of Fig. 4 show the transients obtained by a conventional scanning measurement obtained during the measurement time of 70 min.

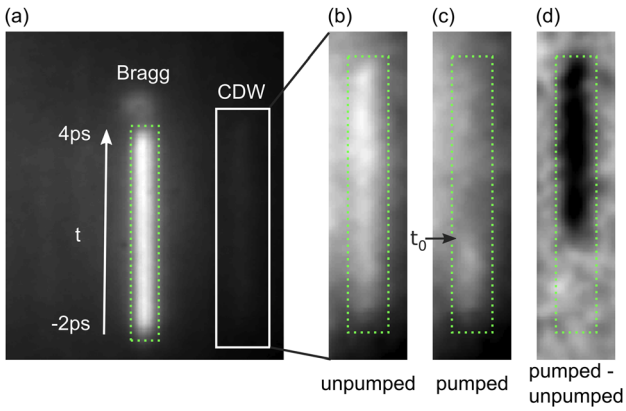

FIG. 3. Panel (a) shows the averaged streak of all available Bragg peaks. The much weaker CDW streaks are not visible due to the intensity scaling of the image. With an adjusted intensity scaling one of the six CDW streaks is displayed in panel (b) with panel (c) indicating the CDW streak with the pump beam on, t_0 is clearly visible. Panel (d) shows the pumped and unpumped images subtracted from each other.

In order to determine whether streaked electron diffraction can compete with the conventional scanning technique, we need to consider three aspects: (i) temporal resolution, (ii) observable time-window per measurement, and (iii) SNR of the measurement.

(i) In conventional scanning electron diffraction the temporal resolution is determined by the convolution of the optical pump pulse and the electron probe pulse and is in our case ~400 fs. On the other hand, in streaked electron diffraction the temporal resolution is determined by the optical pump pulse duration $\Delta\tau_o = 200$ fs, the streak camera's temporal resolution $\Delta\tau_s$, and the temporal jitter $\Delta\tau_j$ between the streaking field and the electron pulse arrival. Here, $\Delta\tau_j < 100$ fs as our photo-triggered streak camera relies on optical rather than electronic synchronization.[12] The temporal resolution of the streak camera is given by the ratio of the width (FWHM) of the unstreaked diffracted beam and the

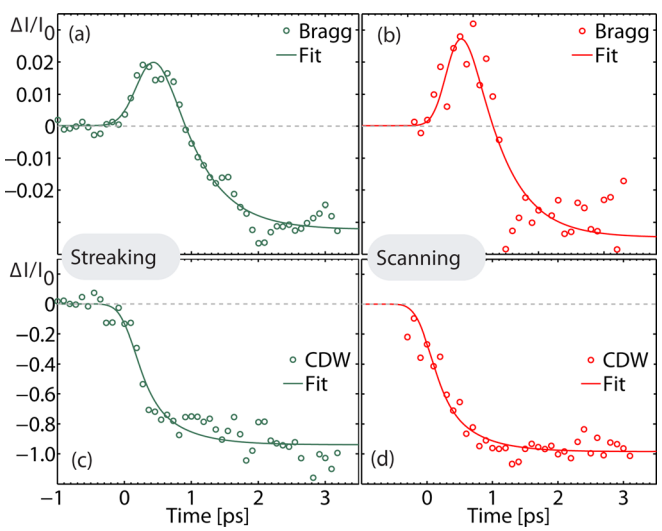

FIG. 4. Comparison of transients obtained by streaking (data acquisition time 60 min, fluence of 3 mJ/cm^2) and scanning methods (data acquisition time 70 min, fluence of 2.6 mJ/cm^2). Although the streak length was ~6 ps, only 4 ps are plotted for direct comparison. The streak data were binned with a 100 interval, i.e., 3 data points were averaged, for better comparability to the scanned data. The fit model (solid lines) is briefly outlined in the text and elaborated in Ref. 8.

streak length, governed by the streak velocity. The streak velocity is directly determined by measuring the electron beam deflection vs. arrival time of the photo-switch trigger pulse. In the present configuration $\Delta\tau_s = 500$ fs. Thus, including $\Delta\tau_j$ and $\Delta\tau_o$, the overall temporal resolution of the experiment is $\Delta\tau \approx 550$ fs.

(ii) The observable time-window of the transient is determined by the temporal length of the incoming electron pulse but cannot be increased arbitrarily. Individual streaks of two adjacent diffraction spots should not overlap on the detector (Fig. 2), setting up an upper boundary for the time window. This condition can be relaxed if the sample is rotated in such a way that the vertical streaks will pass next to each other as is the case in Fig. 2(b). For the given electron beam parameters and lattice constants of 4 H_b-$TaSe_2$ a chosen time window of 6 ps is feasible. Longer time dynamics can, however, easily be studied if the electron pulse is prolonged and the streaking velocity accordingly reduced. This results in a reduced temporal resolution, which however is not really required for slower, long timescale dynamics.

(iii) In order to compare the SNR of both methods, we refer to the data displayed in Fig. 4. Let us directly compare the obtained transients for the Bragg dynamics, shown in Figs. 4(a) and 4(b). For the streaking experiment, $\sim 2 \times 10^4$ electrons per pulse were used, 30 images taken (exposure time 120 s, each), and 13 streaks were superimposed. In the scanning experiment, $\sim 1.5 \times 10^3$ electrons per pulse, 70 images (exposure time 60 s, each), and 15 reflections were used. Thus, in the streaking experiment five times more electrons were collected during roughly the same acquisition time and for the same length of the transient of 3 ps. Since the streak camera resolution is the same as the scanning method, the expected increase in SNR will be by a factor of $\sqrt{5} = 2.2$. This estimate can be directly compared to the experimentally obtained SNR $= \frac{A_S}{\sigma_N}$, with A_S being the amplitude of the signal and σ_N being the standard deviation of the noise. As signal amplitudes A_S for the streaking and the scanning experiment are nearly the same, SNR is governed by σ_N. By subtracting the fitted curve from the measured data, the remainder represents the noise, from which σ_N can be determined. For the two curves, $\sigma_{streaking} = 0.003$ and $\sigma_{scanning} = 0.011$ is extracted, demonstrating an increase in SNR by a factor of $\sigma_{scanning}/\sigma_{streaking} \approx 3.7$. The SNR is not improved in the CDW transients shown in Figs. 4(c) and 4(d); the reason for this is that in the streaking experiment only one out of the six satellites could be analyzed (due to overlapping of streaks) compared to all six well separated CDW peaks in the scanning experiment.

The fact that the increase in the SNR of the streaking configuration is higher than expected based on statistics can be attributed to the parallel data acquisition. Here, the entire transient is recorded by each shot. Thus, intensity fluctuations, laser drifts, etc. are effectively averaged out. In fact, in the current configuration we are largely limited by the detector noise. Further improvement of SNR can be achieved by using gated MCP detectors and reducing the background signal due to inelastically scattered electrons and photoelectrons from pumping the sample.

This is the first demonstration of streaking a subrelativistic diffracted electron beam with a photo-triggered

streak camera. Already at this proof-of-principle stage, the streaking experiment outweighs the scanning technique in terms of SNR while almost matching the temporal resolution. However it can quite easily be further improved. First, a resolution on the order of ~250 fs can be achieved by increasing the streaking voltage by 50% and by halving the streak plate separation. These modifications are realistic, avoiding surface tracking across the GaAs photo switches and leaving sufficient free solid angle for accommodating several diffraction orders. Second, a further increase in SNR requires an additional increase in the number of electrons per pulse. In the current experimental configuration, a minimum distance of 3 cm from the cathode to the sample is required. Particle tracking of space charge dominated electron pulses show that 10^6 electrons per pulse yield a 3 ps electron pulse at the sample. This would theoretically yield a SNR increase by a factor of 16. To be able to tune the pulse length independently from the electron density, the photo-cathode can be driven with a stretched UV pulse; thus, starting with a longer electron pulse where the Coulomb strain also in lateral direction is relieved.

In conclusion, we have experimentally demonstrated a novel concept of ultrafast, non-relativistic electron diffraction to study structural dynamics in complex matter. The concept allows for capturing a transient diffraction signal with a high temporal resolution in a single exposure. This is accomplished by inserting a compact, photo-triggered streak camera into the diffracted electron beam path. We experimentally demonstrated a temporal resolution of 550 fs and outlined the way to achieve the time-resolution of 250 fs. The method would be absolutely crucial for studying light-sensitive materials and/or irreversible processes in a single-shot fashion. However, the increase in the signal-to-noise ratio demonstrated here in our case study points out its advantages also for studying reversible phenomena.

This work was based upon research supported by the South African Research Chair Initiative of the Department of Science and Technology and the National Research Foundation. We would like to acknowledge R. Siegmund for his valuable contribution to the streak camera design. M.E. would like to acknowledge financial support through a *Stiftung der Deutschen Wirtschaft* scholarship.

[1]B. J. Siwick, J. R. Dwyer, R. E. Jordan, and R. J. D. Miller, Science **302**, 1382 (2003).
[2]H. Park, X. Wang, S. Nie, R. Clinite, and J. Cao, Solid State Commun. **136**, 559 (2005).
[3]M. Ligges, I. Rajkovic, P. Zhou, and O. Posth, Appl. Phys. Lett. **94**, 101910 (2009).
[4]M. Chergui and A. H. Zewail, ChemPhysChem **10**, 28 (2009).
[5]M. Eichberger, H. Schäfer, M. Krumova, M. Beyer, J. Demsar, H. Berger, G. Moriena, G. Sciaini, and R. J. D. Miller, Nature (London) **468**, 799 (2010).
[6]B. J. Siwick, J. R. Dwyer, R. E. Jordan, and R. J. D. Miller, J. Appl. Phys. **92**, 1643 (2002).
[7]M. Harb, R. Ernstorfer, T. Dartigalongue, C. T. Hebeisen, R. E. Jordan, and R. J. D. Miller, J. Phys. Chem. B **110**, 25308 (2006).
[8]N. Erasmus, M. Eichberger, K. Haupt, I. Boshoff, R. Birmurske, H. Berger, J. Demsar, and H. Schwoerer, Phys. Rev. Lett. **109**, 167402 (2012).
[9]M. Gao, H. Jean-Ruel, R. R. Cooney, J. Stampe, M. de Jong, M. Harb, G. Sciaini, G. Moriena, and R. J. D. Miller, Opt. Express **20**, 12048 (2012).
[10]G. F. Mancini, B. Mansart, S. Pagano, B. van der Geer, M. de Loos, and F. Carbone, Nucl. Instrum. Methods Phys. Res. A **691**, 113 (2012).
[11]G. H. Kassier, N. Erasmus, K. Haupt, I. Boshoff, R. Siegmund, S. M. M. Coelho, and H. Schwoerer, Appl. Phys. B **109**, 249 (2012).
[12]G. H. Kassier, K. Haupt, N. Erasmus, E. G. Rohwer, H. M. von Bergmann, H. Schwoerer, S. M. M. Coelho, and F. D. Auret, Rev. Sci. Instrum. **81**, 105103 (2010).
[13]G. Mourou and S. Williamson, Appl. Phys. Lett. **41**, 44 (1982).
[14]R. Li, W. Huang, Y. Du, L. Yan, Q. Du, J. Shi, J. Hua, H. Chen, T. Du, H. Xu, and C. Tang, Rev. Sci. Instrum. **81**, 036110 (2010).
[15]P. Musumeci, J. T. Moody, C. M. Scoby, M. S. Gutierrez, M. Westfall, and R. K. Li, J. Appl. Phys. **108**, 114513 (2010).
[16]J. Lüdecke, S. van Smaalen, A. Spijkerman, J. L. de Boer, and G. A. Wiegers, Phys. Rev. B **59**, 6063–6071 (1999).